intersection points are primary, a resonance zone is bounded by a Jordan curve and has an exit and an entry set [15]. The area of each of these sets is the geometric flux, the area leaving the resonance zone each iteration of the map. The images of the exit and entry sets and their intersections completely define the transport properties of the resonance zone [16].

Thus, the beginning of a generalization of this theory to higher dimensions is the study of the intersections of codimension-one stable and unstable manifolds for volume-preserving maps.

As is well-known, a transversal intersection of stable and unstable manifolds is associated with the onset of chaos, giving rise to the construction of Smale horseshoes. A widely used technique for detecting such intersections is the Melnikov method. Given a system with a pair of saddles, and a heteroclinic or saddle connection between them, the Melnikov function computes the rate at which the distance between the manifolds changes with a perturbation. The integral of the Melnikov function between two neighbouring primary intersection points is the first-order term in the geometric flux [17, 18].

Most applications of the method are for two-dimensional maps and flows [19–21], though Melnikov methods were developed for three-dimensional incompressible flows in [22], for symplectic maps in [23], and for general -dimension diffeomorphisms in [24]. In this latter

homology of these curves undergoes bifurcations, and that these bifurcations strongly influence the geometric flux.

2. B t r rt

Suppose $f_0 : \mathbb{R}$ $\to$ $\mathbb{R}$ is a diffeomorphism on -dimensional Euclidean space. Often, we will assume that f preserves a volume-form , for example, the standard volume

$$= \mathrm{d}_1 \square \mathrm{d}_2 \square \cdots \square \mathrm{d} \quad .$$

For this form, f is volume-preserving when it has unit Jacobian, $\det(Df) = 1$.

A smooth perturbation of f_0 is a family of functions $f_\varepsilon \equiv f(\cdot, \varepsilon)$ such that $f(\cdot, 0) = f_0$ and $f(\ , \varepsilon)$ is smooth in both variables. We first define a vector field on $\mathbb{R}$ that will be used to measure the motion of an invariant manifold.

D t (rt r t t r). f_ε f_0, X_ε $\square \mathbb{R}$

$$X_\varepsilon(\ ) \equiv \left[\frac{\partial}{\partial \varepsilon} f_\varepsilon(\ )\right]_{=f_\varepsilon^{-1}(\ )} . \tag{1}$$

Perturbation vector fields have some special properties. First, it is easy to see that X_ε is independent of f_0. Second, if one regards X_ε as a time dependent vector field (where time is ε), then $(\varepsilon) = f_\varepsilon(\ )$ is the solution of the initial value problem

$$\frac{\mathrm{d}}{\mathrm{d}\varepsilon} \equiv X_\varepsilon(\ ), \qquad (0) = f_0(\ ).$$

Thus, if we let $F_{,} = f, \circ f^{-1}$, then F represents the flow of the nonautonomous vector field X_ε [27, theorThus,1w of 81 ()Tj/F1 1m2/F1 1(is)]TJ54 -or any point81 ()Tj5.645
6 1 Tf-1.0179 -.976.9ende()Tj6.97387haoint0

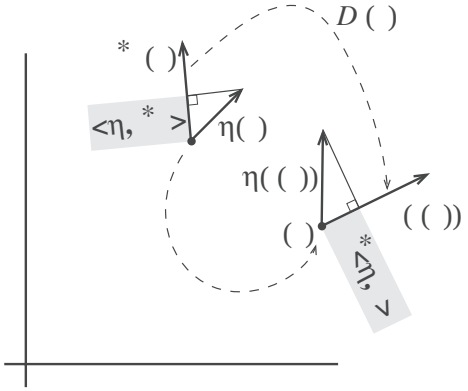

F . r 1. is an adapted normal if the two rectangles shown have the same area.

Adapted normals can be thought of as a generalization of the gradient normal that one gets from a first integral. Recall that the gradient of a smooth function $J : \mathbb{R} \to \mathbb{R}$ is the unique vector field, ∇J, such that for all vector fields Y on $\mathbb{R}$,

$$i_Y \mathrm{d}J \equiv \mathrm{d}J(Y) = \langle \nabla J, Y \rangle. \tag{4}$$

If f has a nondegenerate first integral, $J = J \circ f$, then equation (4) implies that $f^{*}\langle \nabla J, Y \rangle = \langle \nabla (J \circ f), f^{*}Y \rangle$. Therefore, if the diffeomorphism f has a first integral J, then ∇J is an adapted vector field, provided it does not vanish on $\mathcal{W}$.

If we are using the standard inner product on $\mathbb{R}$, then we can characterize adapted normals more concretely.

r t 2. : $\mathcal{W} \to \mathbb{R}$ *m* $\mathcal{W}$,
, , = ′ ⋅ , $\mathbb{R}$. *(3)*
$Y : \mathcal{W} \to \mathbb{R}$, $\mathcal{W}$

$$Df(\ )' \ (f(\ )) = (\ ).$$

In the general case $\mathcal{W}$ is not defined as the level set of an invariant, and it is not easy to

therefore, since $f^{\square} = $, we have

$f^{\square}$

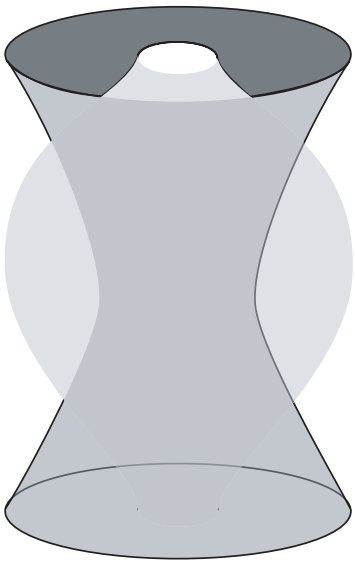

C r ry 7. *m m 6,* ℕ

$$= \circ f_0^- + \sum_{k=0}^{-1} (X_0) \circ f_0^{-k}.$$

, $\lim_{\to\infty} \circ f_0^- ( ) = 0,$

$$( ) = \sum_{k=0}^{\infty} (X_0) \circ f_0^{-k} = \sum_{k=0}^{\infty} ((f_0^{-k})^{\square} X_0). \tag{11}$$

These statements can be directly transcribed for adapted normals using proposition 4.

3.2.

According to theorem 6 and corollary 7, we can compute the Melnikov function (9) in terms of the first-order perturbation vector field X_0. For simplicity, we assume that the perturbation vanishes on the invariant sets.

r t 8. *f m* - $\mathcal{W}$ *m* , *m m* ,

,

Following a standard Melnikov argument based on the implicit function theorem [28], we conclude that if $_0$ is a nondegenerate zero M then near $_0$, the two manifolds W_ε ( ) and W_ε ( ) intersect transversely. □

In a more general version of proposition 8, we would need to drop the condition that X 0d1i04.6(un3.6bler004.6(28.6746 T(W)16 -(bd1 i04.6(th8 16704.6(it TD04.6(/F1 9738 we)-8.3(T*f)-betwe738 1863589738 430.186358successi)3f)10(out.18635837 Tst.1863

r t 12. , - $m\ \Phi$
$\Phi =$ d .

r . This is a straightforward calculation using lemma 10 and proposition 9. □

4.2. F m m

Our goal in this section is to find a compact subset of the manifold—a fundamental domain—that generates the entire manifold under iteration by f_0. We will integrate the flux-form over the fundamental domain to show that the algebraic flux crossing the separatrix is zero. From this point on, we will concentrate on the three-dimensional case. To define the fundamental domain we start with the concept of a proper loop.

D t (r r). $f_0 : \mathbb{R}^3 \to \mathbb{R}^3$ m m, $\mathcal{W}$
. m □ $\mathcal{W}$ $\mathcal{W}$
$\mathcal{W}$ □ int ($\mathcal{W}$) :
$f(cl(\mathcal{W}\ ))$ □ int ($\mathcal{W}\ $).

Similarly, a loop is proper for a backward invariant surface if it is a proper loop for the map f^{-1}.

It is important to notice that not all invariant surfaces admit proper boundaries. A trivial observation is the following proposition.

r t 13. $\mathcal{W}$, $f(\ )$. ,
$\mathcal{W}_{f(\ )} = f(\mathcal{W}\ )$.

The situation that we have in mind relates to the structure of stable and unstable manifolds. Let a, b be compact, normally hyperbolic invariant sets of f, and $\mathcal{W} = W\ (a) = W\ (b)$ a saddle connection between them. A proper loop □ $\mathcal{W}$ is a submanifold of $\mathcal{W}$ that bounds a local submanifold that is an isolating ri-and

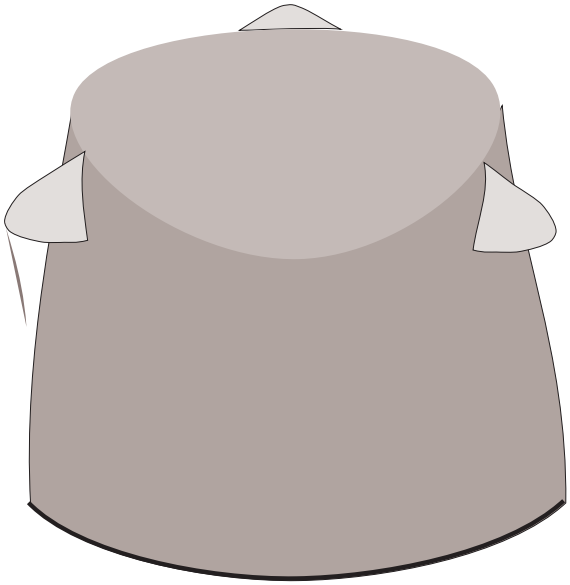

Heteroclinic intersections 80f9etweenic variantic1587

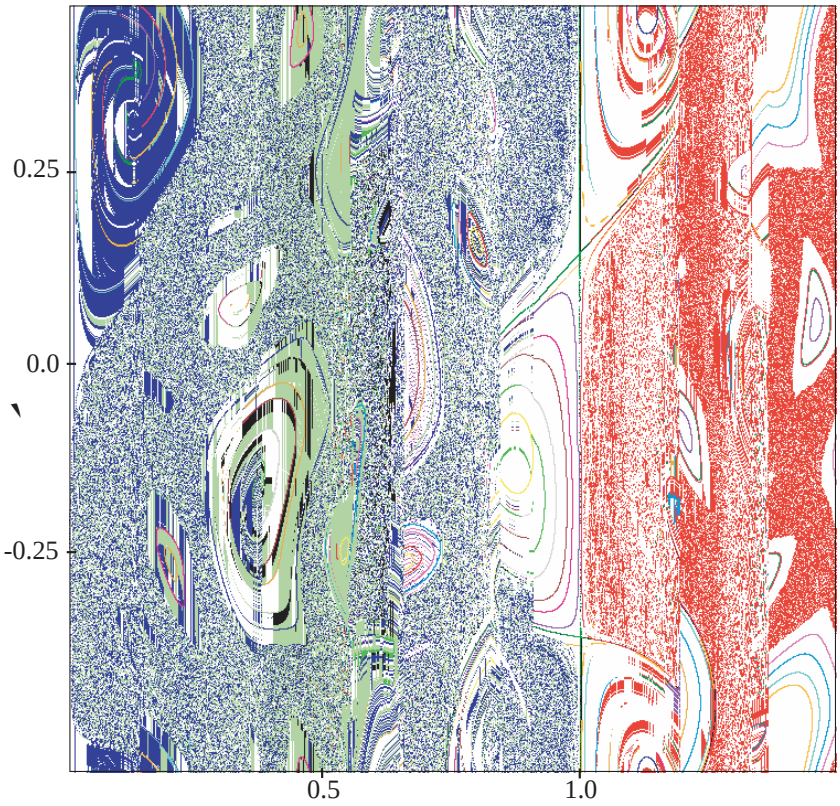

F . r 5. Dynamics of G when h is given by the Arnold circle map with $k = 0.9$. The domain of the figure is $[0, 1.5] \times [-0.5, 0.5]$.

Note that since R and g both preserve , so does f.

The map f still has a rotational symmetry

$$f \circ R = R \circ f \tag{20}$$

for any constant $\in \mathbb{R}$. This implies that when G has a saddle connection, so does f.

r t 16. *(15) (19).* , $\mathcal{W}_0$ $\mathcal{W}_1$

$$\mathcal{C}( ) = \{(, ,): = , = \},$$

h.

Every point on the circles $\mathcal{C}( )$ is fixed under g. The derivative of g at such points is

$$Dg(, ,) = \begin{pmatrix} \frac{1}{2 }(^{-1} \ ^2 + \ ^2) & \frac{1}{2 }(^{-1} - 1) & 0 \\ \frac{1}{2 }(^{-1} - 1) & \frac{1}{2 }(^2 + \ ^{-1} \ ^2) & 0 \\ & = & \end{pmatrix}$$

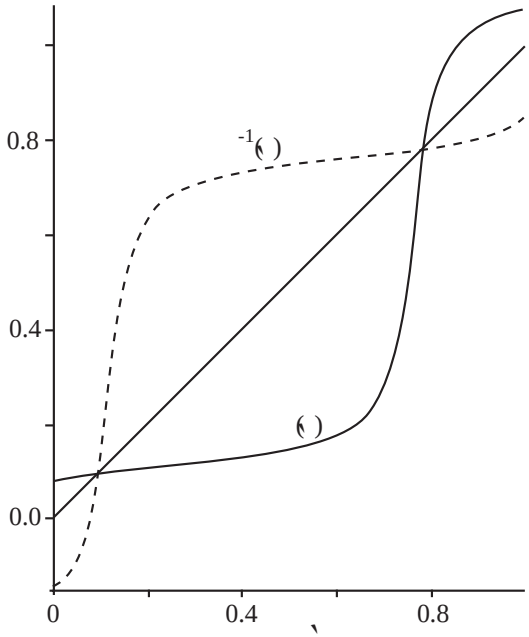

F . r 6. The circle map $h_m(\ )$

There are several such bifurcations in homology type of the zero contours as we vary the parameters. For example, in the upper left panel, the homology type is $(3, 1)$— as each zero contour moves from the bottom to the top of $\mathcal{P}$, it lags the maps translation of by a full circuit in three vertical transits. In the top-right panel there are two zero contours with the homology $(2, 1)$. To elucidate these changes in homology, we show a bifurcation diagram in the space of the parameters in figure 9. We have only found the three homology classes already mentioned.

Also shown in figure 9 are contours of the first-order geometric flux

$$\text{Flux} = \frac{1}{2}\int_{\mathcal{P}} |\Phi|$$

as a function of and . The flux is largest when and are both small, and it appears to get extremely small as approaches one. Note that there is a 'valley' in the flux contours near both homology bifurcations.

Finally, we have also studied the perturbation

$$\begin{aligned} P_1(\ ,\ ,\ ) &= ((1+\ ^2)(\ ^{\square 2} - \ ^2), 0, 0), \\ P_2(\ ,\ ,\ ) &= (0,\ ^2(\ ^{\square 2} - \ ^2), 0), \\ P_3(\ ,\ ,\ ) &= (0, 0,\ - \ ^{\square}), \end{aligned} \tag{28}$$

giving a perturbation vector field $X_0 = P_1 + P_2 + P_3$. We show the bifurcation diagram for the zero contours of $M_{\mathrm{d}J}$ for $\mathcal{W}_0$ in figure 10. For this case, there appear to be only two homology types, $(1, 0)$ and $(3, 1)$. Again there is a 'valley' in the flux near the bifurcation curve.

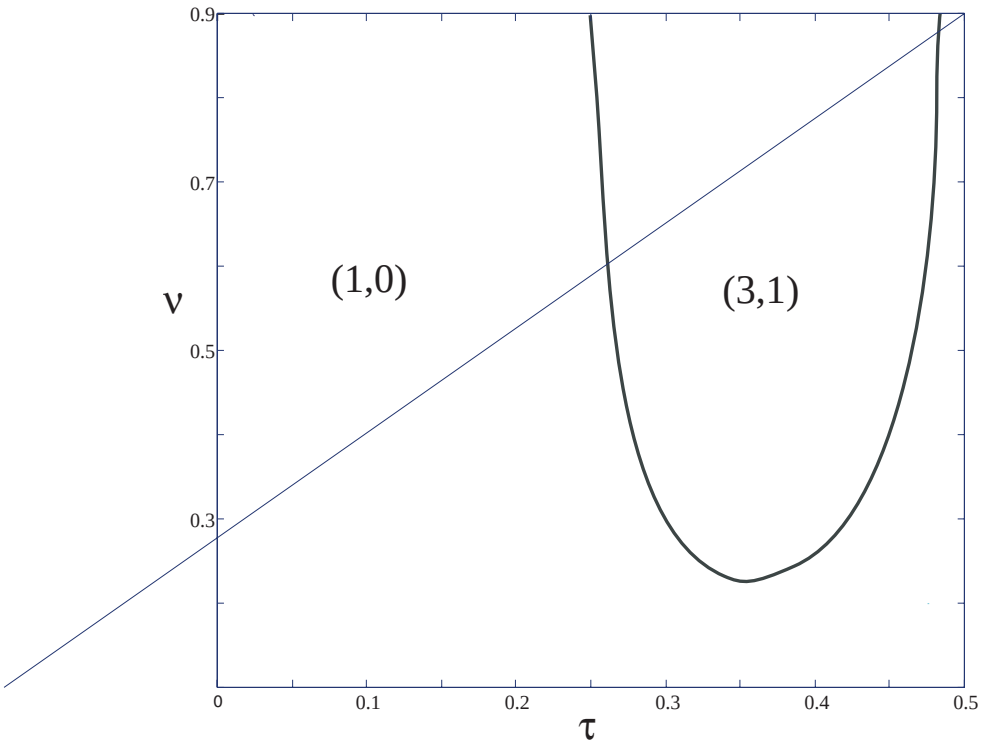
0.9
0.7
0.5
0.3
ν
(1,0)
(3,1)
0
0.1
0.2
0.3
0.4
0.5
τ

[1] Holmes P 1984 Some remarks on chaotic particle paths in time-periodic, three-dimensional swirling flows *C m* . .